

Hard- Pomeron behavior of the Longitudinal Structure Function F_L in the Next- to- Leading- Order at low x

G.R.Boroun*

Physics Department, Razi University, Kermanshah 67149, Iran

(Dated: June 16, 2021)

We present an analytic formula to extract the longitudinal structure function in the next- to -leading order of the perturbation theory at low x , from the Regge-like behavior of the gluon distribution and the structure function at this limit. In this approach, the longitudinal structure function has the hard- Pomeron behavior. The determined values are compared with the $H1$ data and MRST model. All results can consistently be described within the framework of perturbative QCD which essentially show increases as x decreases.

1 Introduction

The longitudinal structure function $F_L(x, Q^2)$ comes as a consequence of the violation of Callan- Gross relation [1] and is defined as $F_L(x, Q^2) = F_2(x, Q^2) - 2xF_1(x, Q^2)$, Where $F_2(x, Q^2)$ is the transverse structure function. As usual x is the Bjorken scaling parameter and Q^2 is the four momentum transfer in a deep inelastic scattering process. In the quark parton model (QPM) the structure function F_2 can be expressed as a sum of the quark-antiquark momentum distributions $xq_i(x)$ weighted with the square of the quark electric charges e_i : $F_2(x) = \sum_i e_i^2 x(q_i(x) + \bar{q}_i(x))$. For spin $\frac{1}{2}$ partons QPM also predicts $F_L(x) = 0$, which leads to the Callan- Gross relation.

The naive QPM has to be modified in QCD as quarks interact through gluons, and can radiate gluons. Radiated gluons, in turn, can split into quark- antiquark pairs (sea quarks) or gluons. The gluon radiation results in a transverse momentum component of the quarks. Thus, in QCD the longitudinal structure function is non- zero. Due to its origin, F_L is directly dependent to the gluon distribution in the proton and therefore the measurement of F_L provides a sensitive test of perturbative QCD [2]. The next- to- leading order (NLO) corrections to the longitudinal structure function are large and negative, valid to be at small x [3-5].

At small x , the longitudinal structure function can be related to the gluon and sea- quark distribution. In principle, the data on the singlet part of the structure function F_2 constrain the sea quarks and the data on the slope $\frac{dF_2}{d\ln Q^2}$ determine the gluon density [6-10]. One of the most striking discoveries at HERA is the steep rise of the proton structure function $F_2(x, Q^2)$ with decreasing Bjorken x [11]. The behavior of the structure function at small x is driven by the gluon through the process $g \rightarrow q\bar{q}$. Therefore the gluon distribution is observed that governs the physics of high energy processes in QCD. HERA shows that the steep inelastic

*boroun@razi.ac.ir

structure function $F_2(x, Q^2)$ has a steep behavior in the small x region ($10^{-2} > x > 10^{-5}$), even for very small virtualities ($Q^2 \approx 1 \text{ GeV}^2$). This steep behavior is well described in the framework of the DGLAP [12] evolution equations. So, we restrict our investigations to the Regge- like behavior for the gluon distribution and the structure function by the following forms:

$$F_2(x, Q^2) = xS \sim A_S x^{-\lambda_S}, \quad (1)$$

and

$$xg(x, Q^2) = A_g x^{-\lambda_g}. \quad (2)$$

The singlet part of the structure function is controlled by Pomeron exchange at small x , where λ_S is the Pomeron intercept minus one. The exponent was rapid rise in Q^2 of the structure function at this limit. This steep behavior of the structure function generates a similar steep behavior of the gluon distribution at small x , where $\lambda_S \neq \lambda_g$ in next- to- leading order analysis. We also note that λ_g is the Pomeron intercept minus one and rises with Q^2 [10,13-15]. A set of formula to extract the gluon and the structure function exponents was given in [15]. For our calculations, We neglecting of the quark singlet part. So that, the DGLAP equation for the gluon evolution in the NLO can be written as:

$$Q^2 \frac{\partial G}{\partial Q^2} = \frac{\alpha_s}{2\pi} \int_x^1 [P_{gg}^1(z) + \frac{\alpha_s}{2\pi} P_{gg}^2(z)] G(\frac{x}{z}, Q^2) dz, \quad (3)$$

where $P_{gg}^1(z)$ and $P_{gg}^2(z)$ are the LO and NLO Altarelli- Parisi splitting kernels [12]. The running coupling constant $\alpha_s(Q^2)$ has the approximate analytical form in NLO:

$$\frac{\alpha_s(Q^2)}{2\pi} = \frac{2}{\beta_0 \ln(\frac{Q^2}{\Lambda^2})} [1 - \frac{\beta_1 \ln \ln(\frac{Q^2}{\Lambda^2})}{\beta_0^2 \ln(\frac{Q^2}{\Lambda^2})}], \quad (4)$$

where $\beta_0 = \frac{1}{3}(33 - 2N_f)$ and $\beta_1 = 102 - \frac{38}{3}N_f$ are the one- loop (LO) and the two- loop (NLO) correction to the QCD β - function, N_f being the number of active quark flavours ($N_f = 4$). Inserting the splitting kernels $P_{gg}^1(x)$ and $P_{gg}^2(x)$ at the small x limit and carrying out the integration, we obtained [15] an expression for λ_g as follows:

$$\begin{aligned} & \ln \frac{\lambda_{g_0}}{\lambda_g - x^{\lambda_g} \int_{t_0}^t x^{-\lambda_g} (\frac{3\alpha}{\pi} - \frac{61\alpha^2}{9\pi^2}) dt} \\ &= \int_{t_0}^t (\frac{3\alpha}{\pi} - \frac{61\alpha^2}{9\pi^2}) \frac{1 - x^{\lambda_g}}{\lambda_g} dt. \end{aligned} \quad (5)$$

Where $\lambda_{g_0} (= \frac{\partial \ln G(x, t_0)}{\partial \ln \frac{1}{x}})$ is the exponent at the starting scale t_0 while $G(x, t_0)$ is the input gluon distribution.

Also, to find an analytic solution for the singlet structure function exponent, we note that the gluon term is dominate over the scaling violation of F_2 at small- x . Neglecting the quark, the DGLAP evolution equation for the singlet structure function has the form:

$$\frac{dF_2^S}{dt} = \frac{\alpha_s}{2\pi} \int_x^1 dz (2N_f P_{qg}^1(z) + \frac{\alpha_s}{2\pi} P_{qg}^2(z)) G(\frac{x}{z}, Q^2). \quad (6)$$

where $P_{qg}^1(z)$ and $P_{qg}^2(z)$ are the LO and NLO Altarelli- Parisi splitting kernels [1,12]. After substitution and rearrangement these equations, we obtained [15]:

$$\begin{aligned} \lambda_S F_2(x, t) - \lambda_{S_0} F_2(x, t_0) = & \frac{0.555}{\pi} \int_{t_0}^t \alpha_s G(x, t) \left[\left(\frac{2\lambda_g}{3 + \lambda_g} (1 - x^{3+\lambda_g}) + \frac{\lambda_g}{1 + \lambda_g} (1 - x^{1+\lambda_g}) \right. \right. \\ & \left. \left. - \frac{2\lambda_g}{2 + \lambda_g} (1 - x^{2+\lambda_g}) \right) + (2x^{3+\lambda_g} + x^{1+\lambda_g} - 2x^{2+\lambda_g}) \right] dt \\ & + \frac{1.852}{\pi^2} \int_{t_0}^t \alpha_s^2 G(x, t) dt \end{aligned} \quad (7)$$

which defines the solution for λ_S . In this equation $\lambda_{S_0} = \frac{\partial \ln F_2(x, t_0)}{\partial \ln \frac{1}{x}}$ and $F_2(x, t_0)$ is input structure function at the starting scale t_0 .

Based on these results, we concentrate on the hard- Pomeron in our calculations and present an approximation analytical solution for the longitudinal structure function in the NLO corrections. We test its validity comparing it with that of H1 data [8], Donnachie & Landshoff [16], MRST[17-19] and attempt to see how the predictions for longitudinal structure function are compared with the experimental data[8].

We specifically consider the next- to- leading- order (NLO) corrections to the longitudinal structure function F_L , projected from the hadronic tensor by combination of the metric and the spacelike momentum transferred by the virtual photon ($g_{\mu\nu} - q_\mu q_\nu / q^2$). In the next- to -leading order the longitudinal structure function is proportional to hadronic tensor as follows:

$$F_L(x, Q^2)/x = \frac{8x^2}{Q^2} p_\mu p_\nu W^{\mu\nu}(x, Q^2), \quad (8)$$

where p^μ (p^ν) is the hadron momentum and $W^{\mu\nu}$ is the hadronic tensor. In this relation we neglecting the hadron mass.

The basic hypothesis is that the total cross section of a hadronic process can be written as the sum of the contributions of each parton type (quarks, antiquarks, and gluons) carrying a fraction of the hadronic total momentum. In the case of deep- inelastic- scattering it reads:

$$d\sigma_H(p) = \sum_i \int dy d\hat{\sigma}_i(y, p) \Pi_i^0(y), \quad (9)$$

where $d\hat{\sigma}_i$ is the cross section corresponding to the parton i and $\Pi_i^0(y)$ is the probability of finding this parton in the hadron target with the momentum fraction y . Now, taking into account the kinematical constraints one gets the relation between the hadronic and the partonic structure functions:

$$f_j(x, Q^2) = \sum_i \int_x^1 \frac{dy}{y} f_j\left(\frac{x}{y}, Q^2\right) \Pi_i^0(y) = \sum_i f_j \otimes \Pi_i^0(y) \quad , j = 2, L, \quad (10)$$

where $f_j(x, Q^2) = F_j(x, Q^2)/x$. Equation (10) expresses the hadronic structure functions as the convolution of the partonic structure function, which are calculable in perturbation

theory, and the probability of finding a parton in the hadron which is a nonperturbative function. So, in correspondence with Eq.(10) one can write Eq.(8) by follows:

$$F_L/x = \frac{\alpha}{4\pi}[\mathbf{f}_{L,q}^{(1)} \otimes (q_S^0 + q_{NS}^0) + \mathbf{f}_{L,G}^{(1)} \otimes g^0] + (\frac{\alpha}{4\pi})^2[\mathbf{f}_{L,q}^{NS(2)} \otimes (q_S^0 + q_{NS}^0) + \mathbf{f}_{L,q}^{S(2)} \otimes q_S^0 + \mathbf{f}_{L,G}^{S(2)} \otimes g^0 + O(\alpha^3)], \quad (11)$$

where q_S^0 and q_{NS}^0 are the singlet and nonsinglet quark distribution. $\mathbf{f}_{L,q}^{(1)}$ and $\mathbf{f}_{L,G}^{(1)}$ are the LO partonic longitudinal structure function corresponding to quarks and gluons, respectively [21]. $\mathbf{f}_{L,q}^{NS(2)}$ is the NLO quark nonsinglet longitudinal structure function, $\mathbf{f}_{L,q}^{S(2)}$ is the NLO quark longitudinal structure function which contributes only to the singlet, and $\mathbf{f}_{L,G}^{S(2)}$ is the NLO gluon longitudinal structure function [20].

We present the expressions, after full agreement has been achieved, in the form of kernels K^i , $i = NS, S$, and g , which give NLO- F_L upon convolution with $F_2 = x \sum_{j=1}^{N_f} e_j^2 (q + \bar{q})_j$, $F_2^S = (\sum_{j=1}^{N_f} e_j^2 / N_f) x \sum_{j=1}^{N_f} (q + \bar{q})_j$, and the gluon distribution g , respectively:

$$F_L(x, Q^2) = \int_x^1 \frac{dy}{y} K^{NS}(\frac{x}{y}, Q^2) F_2(y, Q^2) + \int_x^1 \frac{dy}{y} K^S(\frac{x}{y}, Q^2) F_2^S(y, Q^2) + \int_x^1 \frac{dy}{y} K^G(\frac{x}{y}, Q^2) G(y, Q^2), \quad (12)$$

where $G(x, Q^2) = xg(x, Q^2)$ and e_j are the quark charges and N_f the number of flavors [21]. The kernels have been obtained with the modified minimal- subtraction (\overline{MS}) scheme for the UV regularization combined with the DIS prescription [20].

Based on the Regge-like behavior for the gluon distribution and singlet structure function, let us put Eqs.(1) and (2) in Eq.(12). Thus Eq.(12) is reduced to:

$$F_L(x, Q^2) = \int_x^1 \frac{dy}{y} [K^{NS}(\frac{x}{y}, Q^2) + K^S(\frac{x}{y}, Q^2)] A_S y^{-\lambda_S} + \int_x^1 \frac{dy}{y} K^G(\frac{x}{y}, Q^2) A_g y^{-\lambda_g}, \quad (13)$$

Here the nonsinglet quark density is negligible at small x and the kernels K^i (i =nonsinglet,

singlet and gluon) are defined by:

$$\begin{aligned}
K^{NS}(\frac{x}{y}, Q^2) = & \frac{\alpha_s}{4\pi} 4C_F(x/y)^2 + (\frac{\alpha_s}{4\pi})^2 [4C_F(C_A - 2C_F)(x/y)^2 [8(\frac{1}{2}\ln(1-x/y)^2\ln(+x/y) \\
& + \ln(1-x/y)\text{polylog}(2, 1-x/y) - \text{polylog}(3, 1-x/y) + \zeta(3)) + 4\text{polylog}(3, x/y) \\
& + 4\text{polylog}(3, -x/y) - 4\text{dilog}(1+x/y)(\ln(x/y) - 2\ln(1+x/y)) \\
& - 4\ln(x/y)\text{dilog}(1-x/y) - 2\ln(x/y)^2\ln(1-(x/y)^2) - 8\zeta(3) + 4\ln(x/y)\ln(1+x/y)^2 \\
& + \frac{2}{5}(5-3(x/y)^2)\ln(x/y)^2 - \frac{23}{3}\ln(1-x/y) - 4\frac{2+10(x/y)^2+5(x/y)^3-3(x/y)^5}{5(x/y)^3} \\
& (+\text{dilog}(1+x/y) + \ln(x/y)\ln(1+x/y)) + \frac{2}{3}Pi^2(\ln(1-(x/y)^2) - \frac{5-3(x/y)^2}{5}) \\
& + 4\frac{6-3x/y+47(x/y)^2-9(x/y)^3}{15(x/y)^2}\ln(x/y) - \frac{144+294x/y-1729(x/y)^2+216(x/y)^3}{90(x/y)^2}] \\
& + 8C_F^2(x/y)^2[2\text{dilog}(1-x/y) + \frac{1}{2}\ln(x/y)^2 - \frac{Pi^2}{3} + \frac{41}{6}\ln(x/y) - \frac{5}{3}\ln(1-x/y) \\
& - \frac{96-535x/y}{36x/y}] - \frac{8}{3}C_F N_f(x/y)^2(\ln(\frac{(x/y)^2}{1-x/y}) - \frac{6-25x/y}{6x/y})], \tag{14}
\end{aligned}$$

$$\begin{aligned}
K^S(\frac{x}{y}, Q^2) = & (\frac{\alpha_s}{4\pi})^2 (\frac{16}{9}C_F N_f(3(1-2x/y-2(x/y)^2)(1-x/y)\ln(1-x/y) \\
& + 9(x/y)^2(+\text{dilog}(1-x/y) + \ln(x/y)^2 - Pi^2/6) + 9x/y(1-2(x/y)^2)\ln(x/y) \\
& - 4(1-x/y)^3), \tag{15}
\end{aligned}$$

$$\begin{aligned}
K^G(\frac{x}{y}, Q^2) = & \frac{\alpha_s}{4\pi} [8(x/y)^2(1-x/y)] [\sum_{i=1}^{N_f} e_i^2] + (\frac{\alpha_s}{4\pi})^2 [\sum_{i=1}^{N_f} e_i^2] 16C_A(x/y)^2 (+4\text{dilog}(1-x/y) \\
& - 2(1-x/y)\ln(x/y)\ln(1-x/y) + 2(1+x/y)\text{dilog}(1+x/y) + 3\ln(x/y)^2 \\
& + 2(x/y-2)Pi^2/6 + (1-x/y)\ln(1-x/y)^2 + 2(1+x/y)\ln(x/y)\ln(1+x/y) \\
& + \frac{(24+192x/y-317(x/y)^2)}{24(x/y)}\ln(x/y) + \frac{(1-3x/y-27(x/y)^2+29(x/y)^3)}{3(x/y)^2}\ln(1-x/y) \\
& + \frac{(-8+24x/y+510(x/y)^2-517(x/y)^3)}{72(x/y)^2} - 16C_F(x/y)^2(\frac{5+12(x/y)^2}{30}\ln(x/y)^2 \\
& - (1-x/y)\ln(1-x/y) + \frac{-2+10(x/y)^3-12(x/y)^5}{15(x/y)^3} (+\text{dilog}(1+x/y) \\
& + \ln(x/y)\ln(1+x/y)) + 2\frac{5-6(x/y)^2}{15}Pi^2/6 + \frac{4-2x/y-27(x/y)^2-6(x/y)^3}{30(x/y)^2}\ln(x/y) \\
& + \frac{(1-x/y)(-4-18x/y+105(x/y)^2)}{30(x/y)^2}). \tag{16}
\end{aligned}$$

For the SU(N) gauge group, we have $C_A = N$, $C_F = (N^2 - 1)/2N$, $T_F = N_f T_R$, and $T_R = 1/2$ where C_F and C_A are the color Cassimir operators. In our calculations, we use the Riemann ζ function and the well-known Nielsen generalized polylogarithms, where the

Nielsen's polylogarithm is defined by

$$S_{n,p}(x) = \frac{(-1)^{n+p-1}}{(n-1)!p!} \int_0^1 dt \frac{\ln^{n-1}(t) \ln^p(1-xt)}{t}, \quad (17)$$

In this equation, the values n and p are positive integers and x is complex. Also the ordinary polylogarithm is given in terms of this as [22]:

$$Li_n(x) = S_{n-1,1}(x), n \geq 2. \quad (18)$$

These equations are a set of formulas to extract the longitudinal structure function, using the gluon distribution exponent and the structure function exponent determined in [15] at small x in the next- to- leading order of the perturbation theory.

We computed the predictions for all detail of the longitudinal structure function in the kinematic range where it has been measured by *H1* collaboration [8] and compared with DL model [16] based on hard Pomeron exchange, also compared with computation Moch, Vermaseren and Vogt [17-18] at the second order with input data from MRST [19]. Our numerical predictions are presented as functions of x for the $Q^2 = 12, 15, 20$ and 25 GeV^2 . The average value Λ in our calculations is corresponding to 292 MeV . Results of these calculations are given in Table.1. In Fig.1, the values of the NLO-longitudinal structure functions are compare with the experimental *H1* data[8]. The curves represent the NLO QCD calculations F_L based on a fit to the 1996 – 1997 data. We compare our results with predictions of F_L up to NLO in perturbative QCD [17-18] that the input densities is given by MRST parameterizations [19]. Also, we compare our results with the two pomeron fit as is seen in Fig.1. These results indicate that the complete expression for F_L including the NLO corrections can provide solutions for relevant tests of QCD. The data extend the knowledge of the longitudinal structure function into the region of low- x . This implies that the x dependence of the longitudinal structure function at low x is consistent with a power law, $F_L = A_L x^{-\lambda_L}$, for fixed Q^2 . This behavior is associated with the exchange of an object known as the hard Pomeron. As can be seen in all figures, the increase of our calculations for the longitudinal structure functions $F_L(x, Q^2)$ towards low x are consistent with the NLO QCD calculations.

Based on Regge- like behavior of the longitudinal structure function, we calculate exponent λ_L and compare our results with the experimental results from *H1* Collaboration [8] that given as the derivative of the longitudinal structure function with respect to $\ln \frac{1}{x}$, shows by

$$\lambda_L = \frac{\partial \ln F_L(x, Q^2)}{\partial \ln \frac{1}{x}} \Big|_{Q^2 = \text{cte}}. \quad (19)$$

The result of calculation is shown in Fig.2. In this figure, we show λ_L calculated as a function of Q^2 . Our results show that λ_L is independent of x but has a negative slope with respect to $t [= \ln \frac{Q^2}{\Lambda^2}]$. The result for $A_L(Q^2)$ is presented in Fig.3. The coefficients $A_L(Q^2)$ are dependence of t and increase linearly. Having concluded that the data for F_L require a hard Pomeron component, it is necessary to test this with our results.

In conclusion, in this paper we have obtained an analytic solution for the longitudinal structure function in the next- to- leading order at low x . We found that the Regge

theory can be used to constrain the hard Pomeron exchange to the longitudinal structure function behavior. To confirm the method and results, the calculated values are compared with the $H1$ data on the longitudinal structure function, at small x and QCD fits. These results implies that the NLO contributions improve substantially the agreement with the QCD fit. Thus implying that Regge theory and perturbative evolution may be made compatible at small x . Thus, this behavior at low x is consistent with a dependence $F_L(x, Q^2) = A_L x^{-\lambda_L}$ throughout that region. The longitudinal structure function increase as usual, as x decreases. The form of the obtained distribution function for the longitudinal structure function is similar to the predicted from the proton parameterization, and this is in agreement with the increase observed by the $H1$ experiments. Also, in this paper we have obtained λ_L in the next- to leading order at low x . our results show that the derivatives $\frac{\partial \ln F_L(x, Q^2)}{\partial \ln \frac{1}{x}} = \lambda_L(x, Q^2)$ is independent of x . At low x , the exponent λ_L has a negative slope with respect to t and the coefficient A_L is observed to rise linearly with t . This behavior of the longitudinal structure function at low x is consistent with a power-law behavior.

References

1. G.G.Callan and D.Gross, Phys.Lett.**B22**, 156(1969);
2. R.G.Roberts, The structure of the proton, (Cambridge University Press 1990)Cambridge.
3. A.V.Kotikov, JETP Lett.**59**, 1(1994); Phys.Lett.**B338**, 349(1994).
4. Yu.L.Dokshitzer, D.V.Shirkov, Z.Phys.**C67**, 449(1995).
5. W.K.Wong, Phys.Rev.**D54**, 1094(1996).
6. S.Aid et.al, *H1* collab. phys.Lett. **B393**, 452-464 (1997).
7. R.S.Thorne, phys.Lett. **B418**, 371(1998).
8. C.Adloff et.al, *H1* Collab., Eur.Phys.J.**C21**, 33(2001).
9. N.Gogitidze et.al, *H1* Collab., J.Phys.**G28**, 751(2002).
10. A.V.Kotikov and G.Parente, JHEP **85**, 17(1997); Mod.Phys.Lett.**A12**, 963(1997).
11. C.Adloff,*H1* collab. phys.Lett. **B393**, 452(1997).
12. Yu.L.Dokshitzer, Sov.Phys.JETP **46**, 641(1977); G.Altarelli and G.Parisi, Nucl.Phys.**B 126**, 298(1977); V.N.Gribov and L.N.Lipatov, Sov.J.Nucl.Phys. **15**, 438(1972).
13. M.Gluk, E.Reya and A.Vogt, Euro.J.Phys.**C5**, 461(1998).
14. A.D.Martin, W.S.Strling and R.G.Roberts, Euro.J.Phys.**C 23**, 73(2002).
15. G.R.Boroun and B.Rezaie, Phys.Atom.Nucl.vol.71, No.6, 1076(2008)
16. A. Donnachie and P.V.Landshoff, Phys.Lett.**B533**, 277(2002); Phys.Lett.**B550**, 160(2002);
J.R.Cudell, A. Donnachie and P.V.Landshoff, Phys.Lett.**B448**, 281(1999);
P.V.Landshoff, hep-ph/0203084.
17. A.Vogt, S.Moch, J.A.M.Vermaseren, Nucl.Phys.**B 691**, 129(2004).
18. S.Moch, J.A.M.Vermaseren, A.vogt, Phys.Lett.**B 606**, 123(2005).
19. A.D.Martin, R.G.Roberts, W.J.Stirling,R.Thorne, Phys.Lett.**B 531**, 216(2001).
20. J.L.Miramontes, J.sanchez Guillen and E.Zas, Phys.Rev.**D 35**, 863(1987).
21. D.I.Kazakov, et.al., Phys.Rev.Lett. **65**, 1535(1990).
22. A.Devoto, et.al., Phys.Rev.**D 30**, 541(1984).
23. A.M.Cooper-Sarkar and R.C.E.Devenish, Acta.Phys.Polon.**B34**, 2911(2003).
24. R.K.Ellis , W.J.Stirling and B.R.Webber, QCD and Collider Physics(Cambridge University Press)1996.

TABLE I: The longitudinal structure function terms based on Regge-like behavior.

$Q^2(GeV^2)$	x	$LO - gluon$	$NLO - gluon$	$NLO - singlet$	$LO - nonsinglet$	$NLO - nonsiglet$
12	0.000161	0.429	-0.029	-0.070	0.072	0.025
12	0.000197	0.406	-0.026	-0.066	0.067	0.023
12	0.000320	0.358	-0.019	-0.057	0.059	0.020
15	0.000201	0.431	-0.025	-0.066	0.072	0.024
15	0.000246	0.407	-0.023	-0.062	0.068	0.022
15	0.000320	0.383	-0.019	-0.057	0.063	0.020
20	0.000268	0.384	-0.018	-0.062	0.074	0.023
20	0.000328	0.367	-0.016	-0.057	0.068	0.021
20	0.000500	0.333	-0.012	-0.050	0.060	0.019
25	0.000335	0.383	-0.015	-0.056	0.072	0.022
25	0.000410	0.364	-0.013	-0.052	0.068	0.020
25	0.000500	0.348	-0.010	-0.049	0.064	0.019

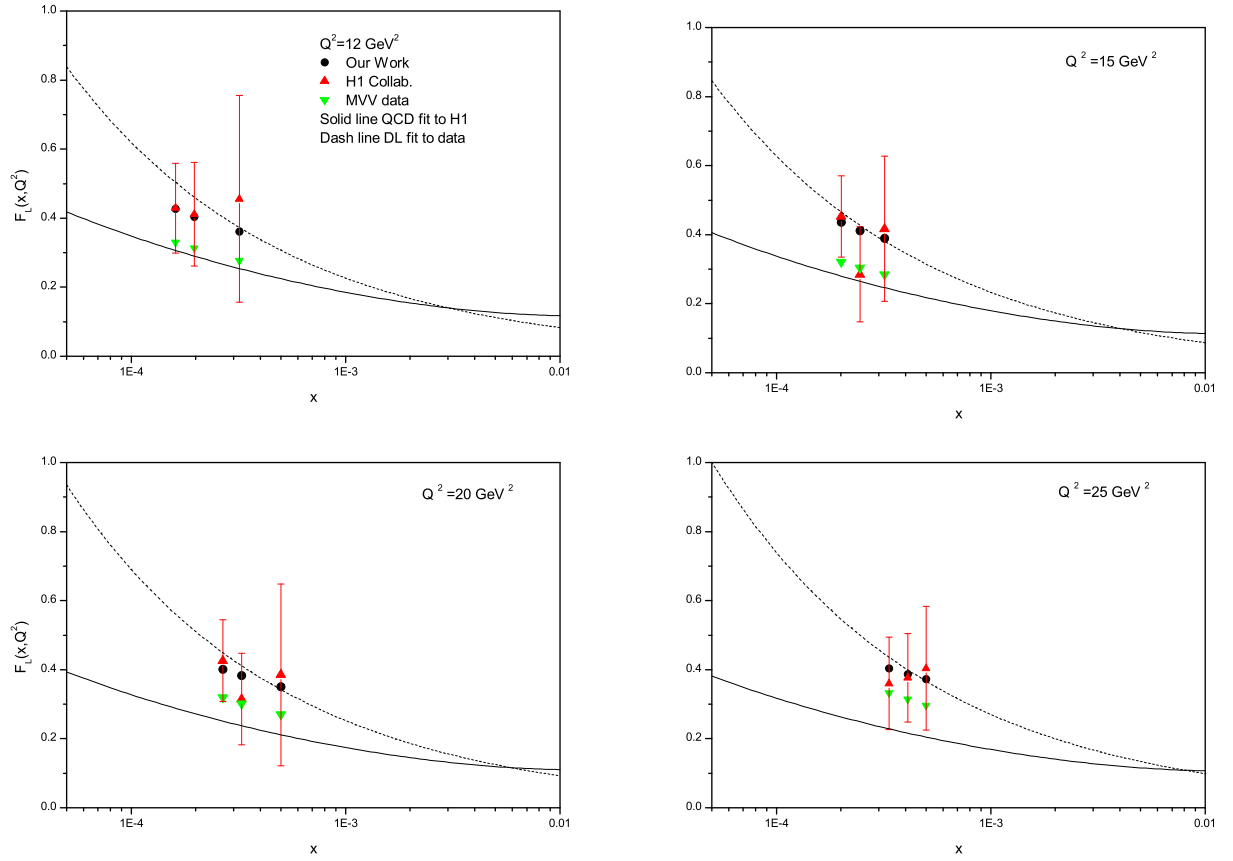


FIG. 1: H1 data [8](up triangle) for the longitudinal structure function at $Q^2=12,15,20$ and 25 GeV^2 values, with our NLO data calculations. The error on the H1 data is the total uncertainty of the determination of F_L representing the statistical, the systematic and the model errors added in quadrature. Down triangle data are the MVV prediction [18]. The solid line is the NLO QCD fit to the H1 data for $y < 0.35$ and $Q^2 \geq 3.5 \text{ GeV}^2$. The dash line is the DL [16] fit to F_L .

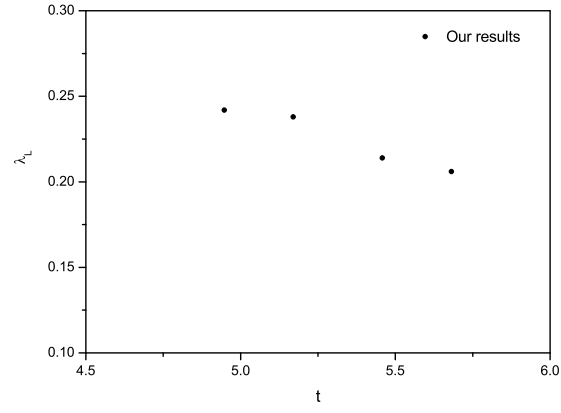


FIG. 2: Calculation of the exponent λ_L from fits of the form $F_L(x, Q^2) = A_L x^{-\lambda_L}$ to our longitudinal structure function data.

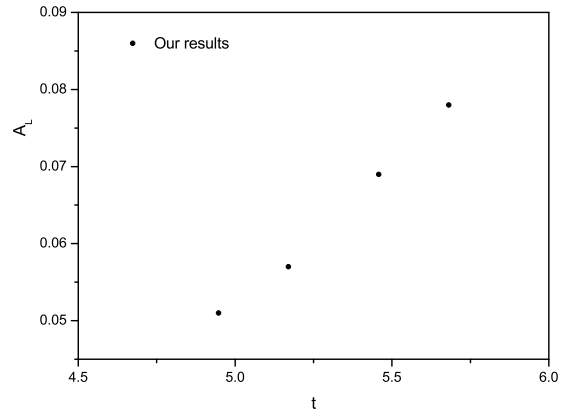


FIG. 3: Calculation of the coefficient A_L from fits of the form $F_L(x, Q^2) = A_L x^{-\lambda_L}$ to our longitudinal structure function data.